ISBN: 978-3-95450-232-5 ISSN: 2673-7000 doi:10.18429/JACoW-NAPAC2022-MOPA08

BEAMLINE OPTIMIZATION METHODS FOR HIGH INTENSITY MUON BEAMS AT PSI

Eremey Valetov*, Paul Scherrer Institut, Villigen PSI, Switzerland
(for the HIMB project)

Abstract

We perform beamline design optimization for the High Intensity Muon Beams (HIMB) project at the Paul Scherrer Institute (PSI), which will deliver muon beams at the unprecedented rate of 10^{10} muons/s to next-generation intensity frontier particle physics and material science experiments. For optimization of the design and operational parameters to maximize the beamline transmission, we use the asynchronous Bayesian optimization package *DeepHyper* and a custom build of *G4beamline* with variance reduction incorporating measured cross sections. We minimize the beam spot size at the final foci using a *COSY INFINITY* model with differential-algebraic system knobs, where we minimize the norms of the respective transfer map components using the Levenberg–Marquardt and simulated annealing optimizers. We obtained a transmission of 1.34×10^{10} muons/s in a *G4beamline* model of the HIMB's particle physics beamline MUH2 into the experimental area.

INTRODUCTION

The muon beamlines at Paul Scherrer Institute (PSI) presently provide muon rates of the order of $\sim 10^8$ muons/s to world-leading intensity frontier muon particle physics experiments and condensed matter research programs. The next generation of these experiments and programs requires a further increase of the muon rates by two orders of magnitude, to the unprecedented level of $\sim 10^{10}$ muons/s [1].

As an example, Mu3e experiment [2] attempts to detect the neutrinoless decay $\mu^+ \to e^+e^+e^-$ of a positive muon into two positrons and one electron. In the Standard Model, this is practically forbidden as this charged lepton flavour violation (cLVF) [3] has a vanishingly small branching ratio of $\sim 10^{-54}$. A positive measurement of $\mu^+ \to e^+e^+e^-$ would provide a clear indication of Beyond-Standard-Model physics. To achieve the sensitivity goal of 10^{-16} with the present rate of $\sim 10^8$ muons/s, Mu3e Phase II would have to run for more than 13 years.

The High Intensity Muon Beams (HIMB) project [4] seeks to deliver muons at $\sim 10^{10}$ muons/s at a proton current of 2.4 mA, making such sensitivities feasible [1].

The MEG II experiment [5], which had its first physics run in 2021, searches for the $\mu^+ \to e^+\gamma$ decay of a positive muon into a positron and a photon. This highly suppressed cLVF process has a branching ratio of also about 10^{-54} in the Standard Model. An increase in the available muon rates will enable a subsequent, next-generation MEG experiment [1] with an improved sensitivity of $O\left(10^{-15}\right)$.

* eremey.valetov@psi.ch

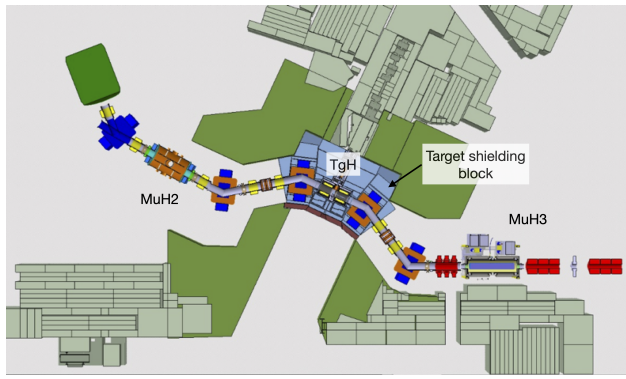

Figure 1: Layout of the HIMB target station and beamlines. The MUH3 beamline is not fully shown; it extends about 38 m from target TgH to the final focus of its branch MUH3.3 and also has a branch MUH3.2.

The muEDM experiment [6], which aims to detect an electric dipole moment of the muon, would also benefit from a novel low-energy, high-brightness muon source coupled to the HIMB [1], compared to using PSI's μE1 beamline. The HIMB could provide a muon beam for muonium spectroscopy measurements that is four orders of magnitude more intensive than the current Low Energy Muons (LEM) beamline at PSI. Other particle physics applications of the HIMB are also envisaged [1].

In addition to particle physics applications, the HIMB will provide faster, higher statistics for measurements using the muon spin rotation method (μSR), enabling novel concepts for sample characterization, including the use of pixel-based detectors or microbeams which require an increase in available muon rate [1].

The HIMB project will achieve the increase of the muon beam intensity by two orders of magnitude to 10^{10} muons/s by replacing the exiting target TgM with a new graphite target TgH with a slanted target design which increases the surface muon rate, high-acceptance capture solenoids close to the target, and transmission using large-aperture solenoids and dipoles. A partial layout of the HIMB is shown in Fig. 1. The particle physics beamline MUH2 has only solenoid focusing, while the materials science beamline MUH3 has solenoid focusing in the first two straight sections and conventional quadrupole focusing further downstream.

This paper expands on our paper [7] on beamline optimization for the HIMB project by detailing the optimization methods aspect of the same work. For broader information about the HIMB project, please refer to the IMPACT conceptual design report (CDR) [4]. The IMPACT project comprises the HIMB and the TATTOOS projects.

ISBN: 978-3-95450-232-5 ISSN: 2673-7000 doi:10.18429/JACoW-NAPAC2022-MOPA08

For optimization of the HIMB beamlines for transmission, we perform asynchronous Bayesian optimizations using the tool *DeepHyper* [8] with objective functions evaluated using the beamline simulation program *G4beamline* [9, 10] and defined as the muon counts at virtual detectors placed along the beamlines, in some cases with adjustments such as weighting of the muon counts as a function of radius. We use *COSY INFINITY* [11] models and the code's built-in Levenberg–Marquardt and simulated annealing optimizers for final focus optimizations, leveraging differential-algebraic transfer maps with system knobs.

We used grid searches for optimizations and studies of the target station TgH with a low number of optimization parameters. In some cases, a comparison was made between the results of optimization using a grid search and *DeepHyper*, with a good agreement. *TRANSPORT*'s [12] built-in optimizer was also used for some beam optics optimizations.

ASYNCHRONOUS BAYESIAN OPTIMIZATION

We perform optimization of the HIMB beamlines for transmission using asynchronous Bayesian optimization on up to 30 Intel Ivy Bridge nodes with 16 cores per node. The main node runs *DeepHyper*'s optimizer, and the evaluation tasks are distributed to the nodes by the workflow manager *Balsam* [13]. The advantage of optimization being asynchronous is that new evaluations are started without waiting for all running evaluations to complete.

Objective function evaluations are performed using a custom build of *G4beamline*. The initial particle ensemble at the target is 50 to 100 thousand muons from a pre-generated beam file, which was obtained by simulating surface muon production using an equivalent of 10^{11} protons impinging on the target, with a splitting factor of 100 for π^+ production and decay. PSI's own measured π^+ cross sections [14] were used, as the measured cross sections were found to be more precise than the default *Geant4* [10] cross sections, which deviated from the experimental data by a factor of up to ten (see Ref. [14]).

The computational intensity of the optimization of the beamlines for transmission results from simulating the beam dynamics with the full beamline geometry and the beam losses on the apertures along the beamlines. We note that the transfer map approach can account for multiple apertures in a lattice model by using a sequence of transfer maps interspersed with aperture exceedance tests; however, the efficiency of this approach decreases as the number of aperture tests is increased for higher simulation accuracy.

We found that, running on 480 cores, asynchronous Bayesian optimization with roughly up to 8 to 10 parameters was effective. Therefore, the optimizations of the beamlines for transmission, especially the MUH3 beamline which is about 38 m long in the model used for the IMPACT CDR, were carried out in stages, starting with optimization of a sufficiently low number of parameters starting from the target station, then successively optimizing parameters corresponding to sections further downstream, with some overlap of parameters.

As expected, optimization was relatively more difficult and required a lower total number of optimization parameters when the latter included quadrupole tuplet fields, for which the optimum is in a long, narrow valley. With the search space only composed of other optimization parameters, such as drift length and solenoid and dipole fields, we did not observe this limitation.

For recent optimizations of the full beamlines or their large sections, we used dipole fields and spatial offsets that were pre-optimized for the passage of a reference particle at the centerline at selected locations in each straight section. While this approach generally does not lead to a global optimum, it was effective because it reduced the number of optimization parameters without any substantial decrease in transmission compared to when these dipole parameters are included in the main, computationally intensive stages of the beamline optimization.

We note that the pre-optimizations of the dipole parameters were done with realistic solenoid or quadrupole fields as much as practicable, and that we kept the possibility of adjusting the dipole parameters in the computationally intensive stages of beamline optimization, e.g., by using a multiplicative coefficient for a dipole field as an optimization parameter, with a small value range in the search space.

We performed numerous optimization studies for the design of the HIMB target station TgH and beamlines MUH2 and MUH3. We also optimized the beamlines MUH2 and MUH3 for transmission. In particular, we achieved a transmission of 1.34×10^{10} muons/s in a model of the MUH2 beamline into the experimental area [7]. Figures 2 and 3 show optimized transmissions in the MUH2 and MUH3 beamlines, respectively, as obtained for the IMPACT CDR. Further design and particle transmission studies are in progress.

OPTIMIZATION USING TRANSFER MAPS WITH SYSTEM KNOBS

We will describe a method that we use for optimization of the final foci using transfer maps with system knobs. The system knobs in this case are parameters such as quadrupole tuplet, magnetic dipole, and horizontal steering magnet fields.

We represent the particle motion using a nonlinear differential-algebraic (DA) transfer map $\mathcal{M}$ such that [15]

$$\vec{z}_\mathrm{f} = \mathcal{M}\left(\vec{z}_\mathrm{i}, \vec{\delta}\right),$$

where $\vec{z}$ is the 2ν phase space coordinates, $\vec{\delta}$ is the system parameters, indices i and f denote the initial and the final state, and ν is the dimensionality of phase space.

To obtain a focused beam in the final state, the horizontal and vertical transverse position components, $\mathcal{M}_x\left(\vec{z}_\mathrm{i}, \vec{\delta}\right)$ and $\mathcal{M}_y\left(\vec{z}_\mathrm{i}, \vec{\delta}\right)$ respectively, are minimized for the beam.

We pick the longitudinal position of the beginning of the final focus where the beam is approximately parallel, for

ISBN: 978-3-95450-232-5 ISSN: 2673-7000 doi:10.18429/JACoW-NAPAC2022-MOPA08

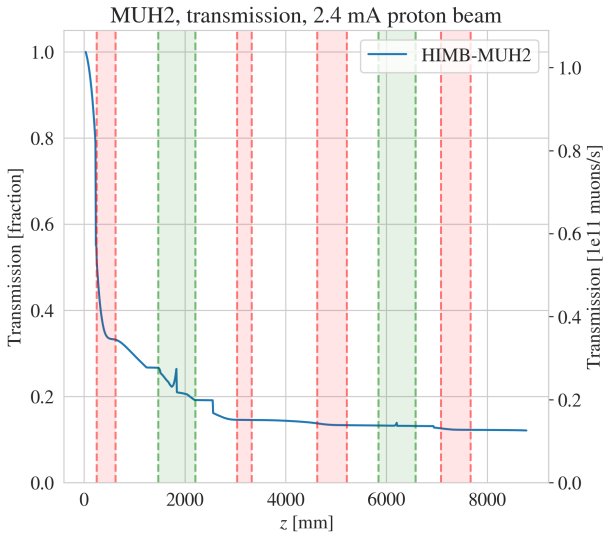

Figure 2: Muon transmission in the MUH2 beamline (preliminary model), plotted vs the longitudinal position. Dipoles and solenoids are denoted by green and red vertical columns, respectively. The optimization of the currents was only for transmission in this case. The vertical spikes at the dipole centers are a *G4beamline* artifact due to a change in the centerline direction.

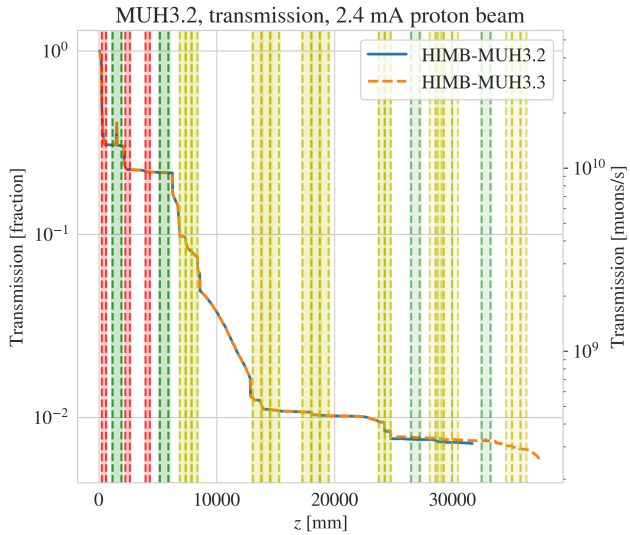

Figure 3: Muon transmission *within the momentum bite* of 25.38 to 29.79 MeV/c to the ends of the MUH3.2 (blue) and MUH3.3 branches (orange) of the MUH3 beamline (preliminary model), plotted vs the longitudinal position. Dipoles, solenoids, and quadrupoles are denoted by green, red, and yellow vertical columns, respectively. The optimization of the currents was only for transmission in this case.

example, in the middle of a somewhat long drift between quadrupole tuplets. We scale the beamline coordinates by the respective half widths of the beam as

$$w_j = z_j / z_{j0},$$

where z_{j0} is the half-width of the beam in coordinate z_j.

For the transfer map $\tilde{\mathcal{M}}\left(\vec{w}_\mathrm{i}, \vec{\delta}\right)$ in the scaled coordinates $\vec{w}$, we consider the summation norms

$$f_{x,y}\left(\vec{\delta}\right) = \left\| \tilde{\mathcal{M}}_{x,y}\left(\vec{w}_\mathrm{i}, \vec{\delta}\right) \right\|_{\vec{w}_\mathrm{i}},$$

where the norms are computed by replacing the expansions in terms of $\vec{w}_\mathrm{i}$ in each $\vec{\delta}$ term by a sum of the absolute values of the coefficients in the same $\vec{\delta}$ term.

Minimization of $f_{x,y}\left(\vec{\delta}\right)$ is done numerically using *COSY INFINITY*'s built-in Levenberg–Marquardt or simulated annealing optimizer. We note that the inverse [15] of f could also be calculated, using the multivariate DA data type of *COSY INFINITY*.

The agreement between our *G4beamline* and *COSY INFINITY* models for the MUH3.2 branch of the MUH3 beamline gave a difference of $\sigma\,(\Delta x) = 1.7$ mm and $\sigma\,(\Delta y) = 3.4$ mm (the latter being larger because of quite long distribution tails) for a beam passing through a quadrupole doublet, a dipole magnet ASS31, and a quadrupole triplet, without collimation at the entrance of the dipole [7]. To put the differences seen between *COSY INFINITY* and *G4beamline* into context, the goal for the beam spot at the final focus is $\sigma_{x,y} \lesssim 20$ mm. The differences of 1.7 and 3.4 mm stated above are thus acceptable.

Recently, we calculated the field of the magnet ASS31 using *COMSOL*'s boundary element method solver, and the current phase of the beamline final focus optimizations is ongoing with this field map.

CONCLUSION

The HIMB beamlines will provide an unprecedented intensity of ~10^{10} muons/s to next-generation muon experiments at PSI. We performed design and beam transport optimizations for the HIMB beamlines using the asynchronous Bayesian optimizer of the tool *DeepHyper* and a custom build of *G4beamline* with variance reduction and utilizing measured π^+ cross sections. DA transfer maps with system parameters computed using *COSY INFINITY* are used for final focus optimizations. We achieved a transmission of 1.34×10^{10} muons/s in a model of the particle physics beamline MUH2 into the experimental area.

ACKNOWLEDGEMENTS

We are thankful to Andreas Knecht, Peter-Raymond Kettle, Angela Papa, Giovanni Dal Maso, and Hubertus Luetkens for productive and interesting discussions. This project has received funding from the European Union's Horizon 2020 research and innovation programme under the Marie Skłodowska-Curie grant agreement No. 884104. This research used resources of the Argonne Leadership Computing Facility, which is a DOE Office of Science User Facility supported under Contract DE-AC02-06CH11357.

ISBN: 978-3-95450-232-5 ISSN: 2673-7000 doi:10.18429/JACoW-NAPAC2022-MOPA08

REFERENCES

[1] M. Aiba *et al.*, "Science Case for the new High-Intensity Muon Beams HIMB at PSI," 2021, arXiv:2111.05788 [hep-ex]. doi:10.48550/arXiv.2111.05788

[2] K. Arndt *et al.*, "Technical design of the phase I Mu3e experiment," *Nucl. Instrum. Methods Phys. Res. A*, vol. 1014, p. 165 679, 2021. doi:10.1016/j.nima.2021.165679

[3] A. de Gouvêa and P. Vogel, "Lepton flavor and number conservation, and physics beyond the standard model," *Prog. Part. Nucl. Phys.*, vol. 71, pp. 75–92, 2013. doi:10.1016/j.ppnp.2013.03.006

[4] R. Eichler *et al.*, "IMPACT conceptual design report," Paul Scherrer Institut, Report No. 22-01, 2022. https://www.dora.lib4ri.ch/psi/islandora/object/psi:41209

[5] A. M. Baldini *et al.*, "The design of the MEG II experiment," *Eur. Phys. J. C*, vol. 78, no. 5, pp. 1–60, 2018.

[6] K. S. Khaw *et al.*, "Search for the muon electric dipole moment using frozen-spin technique at PSI," in *Proc. of The 22nd International Workshop on Neutrinos from Accelerators (NuFact2021)*, vol. 402, 2022, p. 136. doi:10.22323/1.402.0136

[7] E. Valetov, "Beamline Design and Optimisation for High Intensity Muon Beams at PSI," in *Proc. IPAC'22*, Bangkok, Thailand, 2022, paper MOPOTK033, pp. 523–526. doi:10.18429/JACoW-IPAC2022-MOPOTK033

[8] P. Balaprakash, M. Salim, T. D. Uram, V. Vishwanath, and S. M. Wild, "DeepHyper: Asynchronous hyperparameter search for deep neural networks," in *2018 IEEE 25th International Conference on High Performance Computing (HiPC)*, 2018, pp. 42–51. doi:10.1109/HiPC.2018.00014

[9] Muons, Inc., G4beamline, version 3.06. http://www.muonsinternal.com/muons3/G4beamline

[10] S. Agostinelli *et al.*, "Geant4—a simulation toolkit," *Nucl. Instrum. Methods A*, vol. 506, no. 3, pp. 250–303, 2003. doi:10.1016/S0168-9002(03)01368-8

[11] K. Makino and M. Berz, "COSY INFINITY Version 9," *Nucl. Instrum. Methods A*, vol. 558, no. 1, pp. 346–350, 2006. doi:10.1016/j.nima.2005.11.109

[12] U. Rohrer, PSI Graphic TRANSPORT Framework by U. Rohrer based on a CERN-SLAC-FERMILAB version by K. L. Brown *et al.* http://aea.web.psi.ch/Urs_Rohrer/MyWeb/trans.htm

[13] M. Salim, T. Uram, J. Childers, P. Balaprakash, V. Vishwanath, and M. Papka, "Balsam: Automated Scheduling and Execution of Dynamic, Data-Intensive HPC Workflows," in *Proceedings of the 8th Workshop on Python for High-Performance and Scientific Computing*, 2018. doi:10.48550/arXiv.1909.08704

[14] F. Berg *et al.*, "Target studies for surface muon production," *Phys. Rev. Accel. Beams*, vol. 19, no. 2, p. 024 701, 2016. doi:10.1103/PhysRevAccelBeams.19.024701

[15] M. Berz, *Modern Map Methods in Particle Beam Physics*. Academic Press, 1999.